SCIENCE CHINA
Earth Sciences

• RESEARCH PAPER •

February 2012 Vol.55 No.2: 213–220
doi: 10.1007/s11430-011-4358-z

N and O isotopes and the ore-forming mechanism of nitrate deposits in the Turpan-Hami Basin, Xinjiang, China

QIN Yan[1], LI YanHe[1*], LIU Feng[1], HOU KeJun[1], WAN DeFang[1] & ZHANG Cheng[2]

[1] *Key Laboratory of Metallogeny and Mineral Assessment, Institute of Mineral Resource, Chinese Academy of Geological Sciences, Beijing 100037, China;*
[2] *Faculty of Geoscience and Resources, China University of Geosciences, Beijing 100083, China*

Received January 31, 2011; accepted August 23, 2011

The recently discovered nitrate ore field in the Turpan-Hami Basin of western China represents an estimated resource of 2.5 billion tons, and is comparable in scale to the Atacama Desert super-scale nitrate deposit in Chile. The research on this area is rarely carried out, and the origin of the deposits remains uncertain. In this study, new methods were used to systematically analyze N and O isotopes in nitrate minerals collected from the Kumutage, Xiaocaohu, Wuzongbulak, Dawadi, Tuyugou, and Shaer ore deposits in the Turpan-Hami Basin. The data showed that the $\delta^{15}N_{Air}$ value ranges from 0.7‰ to 27.6‰, but mostly between 2‰ and 6‰, which was similar to atmospheric NO_3^-. The ^{18}O was highly enriched with $\delta^{18}O_{V\text{-}SMOW}$ varying from 30.2‰ to 46.7‰. This differs from levels in deposits derived from microbial nitrogen fixation, but is similar to those in atmospheric nitrates. N and O isotopes data indicated that nitrate deposits in Turpan-Hami Basin must be the result of deposition of atmospheric nitrate particles. Although atmospheric nitrate particles are common, the nitrate deposits could form only under the condition of long-term extreme drought climate and very limited biological activity. This paper summarized the ore-forming mechanism of different types nitrate deposits based on their geological setting.

N and O isotopes, nitrate deposits, deposition of atmospheric nitrate particles, Turpan-Haimi Basin

Citation: Qin Y, Li Y H, Liu F, et al. N and O isotopes and the ore-forming mechanism of nitrate deposits in the Turpan-Hami Basin, Xinjiang, China. Sci China Earth Sci, 2012, 55: 213−220, doi: 10.1007/s11430-011-4358-z

Nitrate is an important industrial raw material that is widely used in agriculture, chemical industry, metallurgy, building materials, light industry, medicine, and food products. However, globally, there are very few large nitrate deposits, because nitrate is highly soluble and is easily absorbed and decomposed. Recently, a large deposit of nitrate ore was found in the Turpan-Hami Basin in the Xinjiang of western China. However, previous research in the Turpan-Hami Basin has concentrated on the geology of the area, rather than the isotope geochemistry of the ore deposits. The source and formation process of the nitrate deposits remains unclear. Previous suggestions are diverse, mainly as follows: (1) the formation of nitrate ions via the dissociation of atmospheric nitrogen by lightning [1]; (2) formation from Jurassic coal deposits or other combustible organic matter [2]; and (3) derivation from the area's volcanic rocks [3]. Where the nitrate came from and how it was formed remain unknown.

Sodium nitrate and niter are the commercially valuable constituents of nitrate ore deposits. Stable isotope ratios of nitrogen and oxygen in the nitrate can be used to determine its source and origin. Nitrogen occurs naturally in several different forms (e.g., N_2, NO_x, NH_3, NH_4^+, and NO_3^-). There is an obvious isotope fractionation between different nitrogen sources [4], each having a characteristic $\delta^{15}N$ value [5].

*Corresponding author (email: lyh@mx.cei.gov.cn)

© Science China Press and Springer-Verlag Berlin Heidelberg 2012

The tracing of nitrate sources using a dual isotopic approach, measuring both nitrogen and oxygen, avoids possible ambiguities inherent in methods that rely only on a single isotope. In this study, we used a new method to systematically analyze the δ^{15}N and δ^{18}O values in the nitrate deposits of Kumutage, Xiaocaohu, Wuzongbulak, Dawadi, Tuyugou, and Shaer in the Turpan-Hami Basin. The δ^{15}N-NO_3^- and δ^{18}O-NO_3^- data showed that the nitrate in the Turpan-Hami Basin is formed from the deposition of atmospheric nitrate particles.

The Turpan-Hami Basin is a closed inland basin located in an intermountain depression of the north Tianshan Mountains fold system. It is one of three large intermountain depressions in this region; namely, the Santanghu-Chuomaohu depression to the north, the Turpan-Hami depression of the central region, and the Kumishi depression to the south. The region has a harsh temperate-continental arid climate, with an average annual rainfall of 15 mm, and high rates of evaporation [1, 6]. It is one of the driest areas in the world, and supports little vegetation. Consequently, the area provides ideal conditions for the formation and preservation of nitrate deposits. Strong northwest winds blow all year round, particularly in spring, and gale or even hurricane-force winds are common [7].

The nitrate deposits of the Turpan-Hami Basin lie along the Lan-Xin railway, which covers a distance of more than 400 km from east to west. These ore deposits may be classified into three types [1]. The first is bedrock fissure-filling type of sodium nitrate deposits. They are located in the high foothills, where the bedrock is exposed and fissures are well developed. This bedrock fissure system controls the morphology of the ore bodies, and they tend to be small in scale and few (e.g., Saiergaipu and Tuyugou).

The second is Quaternary alluvial-pluvial, and eluvial, fissure-filling sodium nitrate type of deposits. Deposits of this type are the largest, most widely distributed. They are developed in alluvial and pluvial fans, and in eluvium. The nitrate is usually concentrated at the top of the deposits. The mineralization belts are aligned approximately parallel to the trend of the cordillera, and they are separated by distances >15 km. The surface of the ore body is bare and flat, but tilts (<10°) towards the center of the basin. Saline minerals, such as caliche, fill in the fissures in the Quaternary alluvium and eluvium, cement the gritty sediment, and form a hard salt crust. These gritty sediments are heavily fissured, and have low water content. The mineralized layer is almost exposed outside and has a well-defined vertical structure comprising five distinct zones. Starting with the uppermost and moving downwards, these zones are as follows: (1) grit belt in Gobi, which is 10 cm thick; (2) nitrate belt, in which the grit was cemented by a saline mineral such as caliche, and is about 0.5–1.2 m thick, and nitrate was filled in around the grit or along these fissures; (3) chloride belt, in which cement is mainly halite and nitrate is minor, being 1–2 m thick; (4) sulfate belt, where gypsum is the primary cement, free of nitrate and 0.5–1 m thick; (5) grit belt, with little saline mineral and poor concretion.

The vertical zonation of sodium nitrate deposits reflects the solubility of mineral salts, and follows the typical evaporate-deposit sequence. The vertical distribution of the salts is the opposite to that of the nitrate deposits in the Atacama Desert [8]. The main saline minerals are not only sodium nitrate and niter but also halite, gypsum, pyrotechnite, darapskite, and astrachanite. The nitrate deposits at Kumutage, Xiaocaohu, and Hongtai are representative of this type.

The third type of deposit found in the study area is the modern saline niter type. These deposits contain solid and fluid phases, and formed by chemical precipitation from modern saline. The ore bodies are exposed, and are horizontally bedded in layers of 0.2–1.1 m thick. Potassium nitrate occurs in the salt shell, and liquid potassium nitrate is present in the brine between the mineral crystals. The principal nitrate minerals are niter, soda niter and darapskite are the secondary, and the other saline mineral is halite. Deposits typical of this type are found at Wuzongbulake, Xiaohengshan in the Kumishi intermountain basin, and Dawadi in Tarim Basin. The Kumishi intermountain basin occurred as SEE. There are five dry salt-lakes in there. The Wuzongbulake nitrate deposit is located in the lower Kumishi basin, and the terrain slope is undulating. The ore can be classified as either hard-crust argillo-arenaceous niter or loose argillo-arenaceous niter, with the latter being most abundant. The deposit has a dull appearance and a thin crust. At its base, the deposit is loosely consolidated, wet, and contains a fine sand component. Saline minerals are present towards the base. Dawadi is an intermountain basin, with an area of 12 km^2, and is also of solid-liquid niter deposit.

1 Samples and methods

To determine the geological properties of the nitrate ore deposits at Kumutage, Xiaocaohu, Wuzongbulake, Dawadi, Tuyugou, and Shaer, we collected samples of ore, soil, and water at various locations, and from the three types of mineral deposit outlined above. We then separated the nitrate from the samples, and determined the δ^{17}O, δ^{18}O, and δ^{15}N values of the nitrate.

1.1 Separation and purification of the nitrate

Silva's [9] reformative separation method for nitrate in water was used to separate and purify the nitrate in the ore samples. Sample mass was determined from the likely nitrate content, and the samples were dissolved in 10 mL of deionized water. This solution was then filtered through a 0.45 μm polycarbonate membrane to remove particles that may otherwise have clogged the resin.

To prevent the effect of chloride ions in the solution in-

fluence on the absorption capacity of the ion exchange column, NaCl was removed by recrystallization. Crystallization of most salts (e.g., NaCl) was initiated by heating the filtered solution. Evaporation of the sample volume down to 2 mL resulted in concentration of the nitrate solution, which was further purified by filtering out the NaCl crystals to leave a sufficiently concentrated solution. The nitrate solution was then made up to 20 mL with deionized water. The addition of an eluent of 0.5 mol/L $BaCl_2$ (three times the amount required based on the concentration of SO_4^{2-} in the solution) resulted in the separation of sulfate as $BaSO_4$. The column was left to stand overnight, allowing a stable precipitate to form and the solution to settle. The eluent was then passed through a cation-exchange column (Bio-Rad AG50W-X8) to remove excess Ba^{2+}, and the nitrate-bearing acid eluent was neutralized with Ag_2O, converting the HNO_3 to $AgNO_3$ (eq. (1)). Finally, the pH value was corrected to 5.5–6.0.

$$HCl+HNO_3+Ag_2O=AgCl\downarrow+AgNO_3+H_2O \quad (1)$$

The AgCl precipitate and superfluous Ag_2O were removed by filtration through a 0.25 μm membrane, and the filtrate collected in 100 mL tri-cornered, plastic beakers, which were then directly freeze-dried to obtain solid $AgNO_3$ [9]. The IAEA-NO-3 was used as nitrogen and oxygen isotope reference material isotopes. It was converted to $AgNO_3$ using the same method.

1.2 Analysis of nitrate δ^{15}N

N isotope analysis was performed using a reduction reaction (eq. (2)) of purified $AgNO_3$ with Cu and CuO [10] at 850°C to produce the nitrogen, and δ^{15}N was then determined using an MAT 253 mass spectrometer.

$$2AgNO_3+6Cu=2Ag+N_2\uparrow+6CuO \quad (2)$$

The purified $AgNO_3$ (20 mg) was first weighed into a silver foil capsule, the capsule was then placed into a quartz reaction tube (Figure 1) (9 mm×250 mm), attached to the vacuum system, and vacuumized to 2×10^{-3} Pa. To prevent decomposition of the $AgNO_3$, use opaque to cover the lower part of the reaction tube during process of vacuuming. Valve V1, connected to the reaction tube, was closed, and the tube was placed into the furnace at a preset temperature of 850°C. The reaction was left to progress for 5 minutes at this temperature, and then valves V3, V4, V6, and V7 were closed. Valve V5 was then opened, and the reaction products were fed into a Cu/CuO stove for 30 minutes to ensure that the brown gas was completely removed, and all of the NO_x was converted to N_2. Next, Valve V7 was opened and the gas passed through two liquid-nitrogen cold traps to cryogenically remove any impurities. Valve V9 was closed after 7 minutes, and valve V8 was opened. At last, the N_2 was collected in a calibrated volume finger containing a 5A molecular sieve, N_2 was measured the yield by film gauge and δ^{15}N was determined with an MAT 253 mass spectrometer using the reference material IAEA-NO-3. The δ^{15}N values of the nitrate samples are expressed relative to atmospheric N_2 ($\delta^{15}N_{Air}$) international standards. A laboratory standard sample was measured 18 times, and the 1σ analytical precision for δ^{15}N was 0.18‰.

1.3 Analysis of nitrate δ^{18}O

O isotope analyses were performed on gaseous CO_2 using a reduction reaction of $AgNO_3$ with graphite [9]. The purified $AgNO_3$ was ignited with graphite in a closed tube to produce CO_2, which was then cryogenically purified and analyzed for its oxygen isotope composition. To avoid isotopic exchange between the CO_2 produced during the experiment and the quartz tube, an inner heating method was used and a special quartz reactor developed. The inner heating device

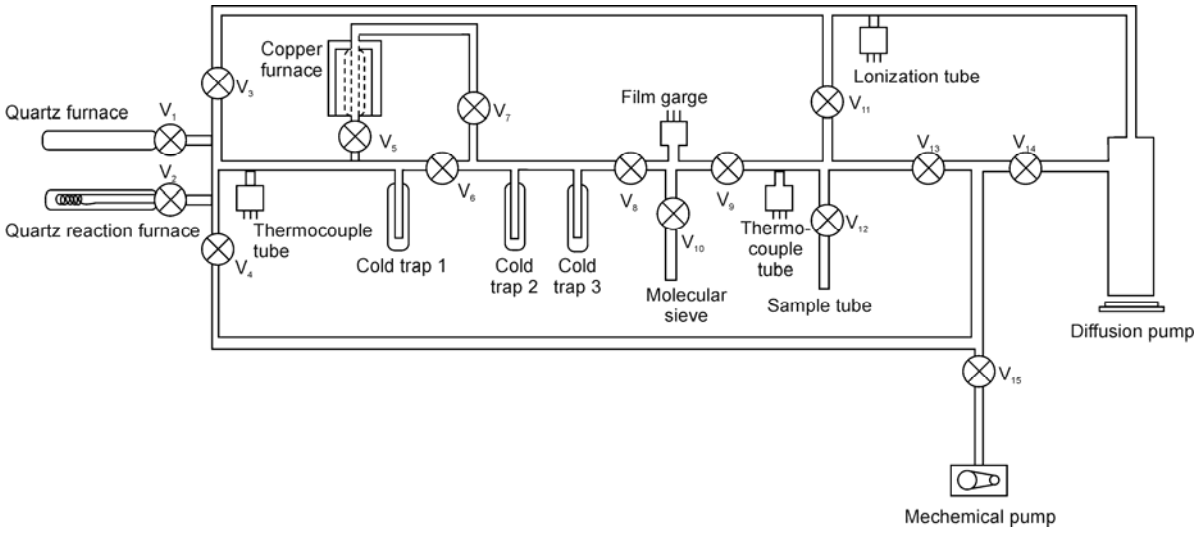

Figure 1 The device of analyzing N and O isotopes of the nitrate.

consists of a platinum insulating layer, a platinum wire heating coil, and a double transformer used to control the temperature.

$$2AgNO_3+3C=2Ag+N_2+3CO_2 \quad (3)$$

The purified $AgNO_3$ (15 mg) and high-purity graphite powder (10 mg) were weighed in a silver foil capsule and then placed in a "platinum boat" for vacuuming to 2×10^{-3} Pa, with reactor valve V2 closed. The sample was quickly heated to 850°C by adjusting the voltage, and was reacted for 1 hour at this temperature. After opening valve V2, we fed the produced gas into the liquid-nitrogen cold trap to freeze the CO_2. The ice-free nitrogen gas was pumped away slowly after 7 minutes. When the required vacuum was achieved, liquid nitrogen was replaced by dry ice-alcohol, and carbon dioxide ice, H_2O, and other impurities were removed. The produced CO_2 was collected in a sample tube using liquid nitrogen, and the $\delta^{18}O$ of the CO_2 was determined with an MAT 253 mass spectrometer, using IAEA-NO-3 as the oxygen isotope reference material. The $\delta^{18}O$ values of the nitrate samples are expressed relative to the Vienna standard mean ocean water (V-SMOW) international standard. A laboratory standard sample, measured 18 times, had a 1σ analytical precision for $\delta^{18}O$ of 0.13‰.

2 Results and discussions

2.1 Nitrogen and oxygen isotopes in the nitrate deposits

Table 1 and Figures 2–5 show the $\delta^{15}N$ and $\delta^{18}O$ values of the nitrate minerals. The NO_3^- samples from the Turpan-Hami Basin nitrate deposits have large variation of $\delta^{15}N$ values (0.7‰–27.6‰), but the majorities are in the range 2‰–6‰ and show an obvious tower effect (Figure 2).

The various types of ore deposits have different $\delta^{15}N$ values (Figure 3). The $\delta^{15}N$ values of the sodium nitrate from Xiaocaohu, Kumutage, Tuyugou, and Shaer were low (0.7‰–6.0‰), and are similar to the values for atmospheric $\delta^{15}N$. Values of $\delta^{15}N$ from the Wuzongbulak niter deposit ranged from 15.0‰ to 27.6‰, which is significantly higher than values of sodium nitrate deposits.

The $\delta^{18}O$ values of the nitrate deposits ranged from 30.2‰ to 47.9‰, but were typically in the range of 40‰–46‰ (Figure 4), which is higher than that of nitrate ions formed by either microbial oxidation (about 10‰) [11, 12] or atmospheric O_2 (23.5‰). The $\delta^{18}O$ values of the Xiaocaohu, Kumutage, Tuyugou, and Shaer sodium nitrate deposits, and the Dawadi niter deposit (35.4‰–46.7‰), are

Table 1 Isotopic value for nitrate from the nitrate deposits in the Turpan-Hami Basin

Sample No.	$\delta^{15}N_{Air}$ (‰)	$\delta^{18}O_{V\text{-}SMOW}$ (‰)
Xiaocaohu sodium nitrate deposit		
XCH-10	3.8	35.4
XCH-11	2.6	
XCH-12	5.3	42.6
XCH-1-W	1.4	
XCH-2	2.8	42.4
XCH-3	3.5	
XCH-4	0.7	
XCH-5	3.7	42.0
XCH-6	1.6	43.1
XCH-7	3.5	43.4
XCH-8	2.1	43.1
XCH-9	4.2	39.3
Shaer sodium nitrate deposit		
Ser-05	2.9	37.3
Tuyugou sodium nitrate deposit		
TYG-03	2.9	42.4
Dawadi niter deposit		
DWD-1	6.1	45.4
DWD-2	5.7	46.0
DWD-3	6.9	45.0
DWD-4	2.9	45.6
DWD-5	5.7	44.9
Kumutage sodium nitrate deposit		
JD-3	2.0	
JD-4	4.6	
KMTG-5	5.3	39.3
KMTG-6	5.4	40.7
KMTG-7	4.9	39.8
KMTG-8	5.2	41.0
KMTG-9	6.0	40.2
QJ7-24C	4.3	39.6
QJ7A27	3.0	43.3
QJ7A27-3	4.3	
QJ7A28	3.6	46.7
QJ7B27-1	2.8	40.0
QJ7B27-2	3.1	38.2
QJ7B27-3		44.9
QJ7B27-4	3.7	41.9
QJ7B27-6	3.3	43.9
QJ7B27-7	2.0	39.0
Wuzongbulake niter deposit		
WZ11	15.0	36.3
WZ12	25.5	31.3
WZ13	24.4	30.3
WZ15	27.6	31.6
WZ17	20.8	30.2

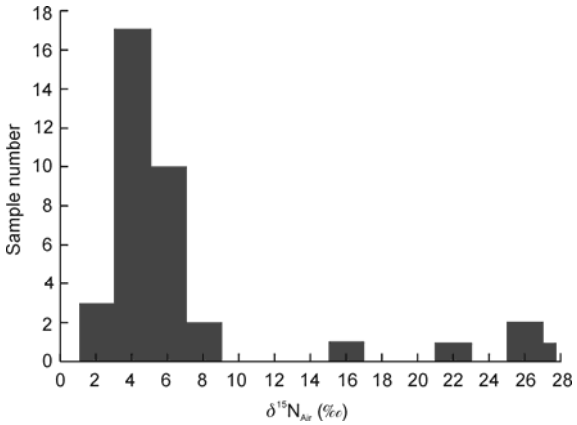

Figure 2 Summary of nitrogen isotope variations in nitrates from the Turpan-Haimi Basin.

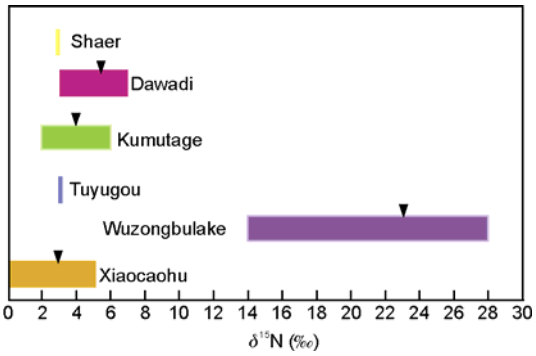

Figure 3 $\delta^{15}N$ varies in different types deposits from the Turpan-Hami Basin. ▼position of mean value.

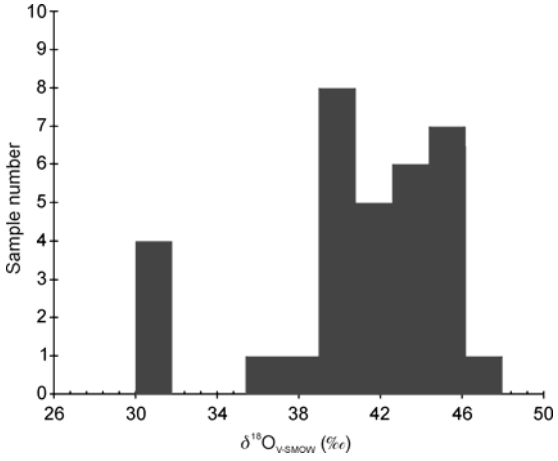

Figure 4 Summary of oxygen isotope variations in nitrates from the Turpan-Haimi Basin.

higher than the values at the other locations. The $\delta^{18}O$ values of the Wuzongbulak niter deposit ranged from 15.0‰ to 27.6‰, and are the lowest in this area (Figure 5).

The isotopic composition is closely related to the type of deposit. The $\delta^{18}O$ values of the sodium nitrate deposits are generally higher, and the $\delta^{15}N$ values are generally lower than values from the niter deposit (Figure 6). The oxygen and oxygen isotopic compositions of sodium nitrate deposits elsewhere are very similar, and do not exhibit any systematic variation with latitude, longitude, or altitude. There were no clear trends in the vertical profiles of $\delta^{18}O$ and $\delta^{15}N$. Compared with the Atacama nitrate deposits, the $\delta^{18}O$ values of sodium nitrate deposits in the Turpan-Hami Basin are lower, and $\delta^{15}N$ values higher. Similarly, when compared with deposits in Death Valley, USA, the $\delta^{18}O$ values of the Turpan-Hami sodium nitrates are clearly higher, and ^{15}N values are slightly higher. The $\delta^{18}O$ and ^{15}N values of the nitrate in Turpan-Hami Basin have a weak anti-correlation.

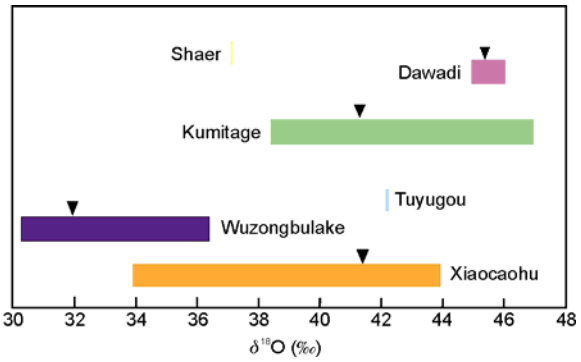

Figure 5 $\delta^{18}O_{V\text{-}SMOW}$ varies in different types deposits from the Turpan-Hami Basin. ▼position of mean value.

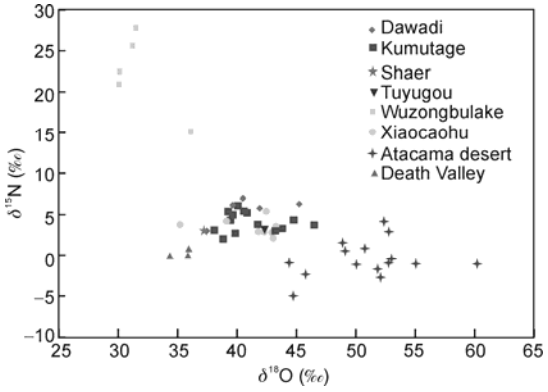

Figure 6 Variation of N and O isotopes in nitrate from the Turpan-Hami Basin, Atacama desert, and Death Valley [13].

2.2 Discussion for origin

The two natural sources of nitrate are microbial nitrification and the production of atmospheric nitrate by photochemical reactions. Microbial nitrification is an important source of nitrate, and the process can be summarized as follows:

$$\text{Organic nitrogen} \rightarrow NH_4^+ \xrightarrow{\text{volatilization of } NH_3} NO_2^- \rightarrow NO_3^- \quad (4)$$

The volatilization of ammonia that accompanies this process causes fractionation of N isotopes. This fractionation strongly enriches ^{15}N in nitrate; levels of $\delta^{15}N$ in ni-

trate formed by microbial nitrification range between 10‰ and 24‰ [14–17]. These values differ significantly from δ^{15}N values in the sodium nitrate deposits of the Turpan-Hami Basin. Nitrate ions formed by microbial oxidation have been shown to contain 2 oxygen atoms from the water, and 1 O atom from the oxygen, present in the oxidizing environment [11, 12, 18–21].

The δ^{18}O value of the NO_3^- may be estimated by

$$\delta^{18}O_{nitrate} = {}^2/_3\delta^{18}O_{water} + {}^1/_3\delta^{18}O_{O_2}. \quad (4)$$

Because the δ^{18}O value of atmospheric oxygen is relatively stable (23.5‰), the δ^{18}O value of nitrate formed by nitrification depends on the oxygen isotopic composition of the local water. The δ^{18}O value of local rainwater and brines ranges from −10‰ to 5‰ [22]. However, the calculated $\delta^{18}O_{V\text{-}SMOW}$ value of nitrate formed by microbial nitrification in the Turpan-Hami Basin is 1‰ to 11‰. This disparity between calculated and measured $\delta^{18}O_{V\text{-}SMOW}$ values indicates that the nitrate in the Turpan-Hami Basin did not form by microbial nitrification. The isotopic composition of nitrogen in the sodium nitrate deposits also supports this interpretation.

Microbial denitrification is an important part of the nitrogen cycle, and can reduce nitrate to N_2O or N_2. This process involves a significant fractionation of O and N isotopes, and results in enriched δ^{18}O and δ^{15}N in the residual nitrate. During Rayleigh fractionation, the values of δ^{18}O and δ^{15}N in the residual nitrate increase exponentially with decreasing nitrate concentration [15, 23]. However, a large amount of experimental data indicates that in microbial denitrification processes, δ^{18}O and δ^{15}N increase at a ratio of 2∶1 with respect to nitrate concentration [24–26]. Lehmann et al. [23] obtained δ^{18}O and δ^{15}N values from residual nitrate formed by denitrification in Lake Lugano, Switzerland, of 27.2‰ and 15.7‰, respectively. The small positive values of $\delta^{15}N_{Air}$ obtained from nitrate in the sodium nitrate deposits from the Turpan-Hami Basin indicate that microbial denitrification did not play a major role in their formation. However, δ^{15}N values from the Wuzongbulake niter deposits were much higher than those obtained from the sodium nitrate deposits, which suggests that microbial denitrification cannot be ignored in the formation of niter deposits here.

Atmospheric nitrate is produced by photochemical reactions involving NO_x and O_3, and OH and H_2O, in the stratosphere and troposphere. The highly chemically active and soluble HNO_3 reacts readily with other materials to form nitrate aerosol particles that are deposited on the surface of the earth by dry- or wet-deposition. Atmospheric nitrate is highly enriched in ^{17}O and ^{18}O, the mass-independent fractionation of oxygen is remarkable [13, 17, 28]. The $\delta^{18}O_{V\text{-}SMOW}$ values of nitrate aerosol from the Dry Valleys of Antarctica are 60‰–111‰, and Δ^{17}O values are 20‰–43‰ [29]. The $\delta^{18}O_{V\text{-}SMOW}$ values of nitrate from rain and snow in northeast Bavaria (Germany) are 53‰–73‰ [20]; similarly, Campbell et al. [30] reported $\delta^{18}O[NO_3^-]$ values of 40‰–70‰ in rainwater from a Colorado suburb. The δ^{18}O values of nitrate minerals obtained from dry valleys in Antarctica, the Atacama Desert in Chile, and Death Valley in America are also unusually high, being 62‰–76‰, 44‰–60‰, and 21‰–46‰, respectively [13, 28]. Atmospheric nitrate and atmospheric nitrogen have similar δ^{15}N values [20, 30], but because of snow re-emissions, atmospheric nitrate in the Polar Regions has an abnormally low value of δ^{15}N, with a large range of −47‰ to 11‰ [28, 29].

The δ^{18}O and δ^{15}N values in the Turpan-Hami Basin are similar to those of nitrate deposits from the Atacama Desert and Death Valley, which were both formed by deposition of atmospheric nitrate aerosols [13, 20, 28–31] (Figure 6). Figure 7 shows the range of δ^{18}O and δ^{15}N values from various sources, and the nitrate deposits from the Turpan-Hami Basin plot within the field that indicates an atmospheric nitrate source. This result implies that the Turpan-Hami nitrates accumulated from the deposition of atmospheric nitrate aerosols. The mass-independent fractionation of oxygen isotopes in these deposits, which occurs in nitrates produced by atmospheric photochemical reactions [32, 33], supports this hypothesis.

Values of δ^{15}N in the Wuzongbulake niter deposits were the highest recorded here (15.0‰–27.6‰), but δ^{18}O values are very low (30.2‰–36.3‰), although still higher than levels from nitrate formed by microbial nitrification. This finding indicates that both the sodium nitrate and niter deposits have the same nitrate source: atmospheric aerosols. Microbial denitrification involves a significant fractionation of oxygen and nitrogen isotopes, and the residual nitrate is relatively enriched in ^{18}O and ^{15}N [15, 23]. Experimental studies of the biological denitrification process [34] indicated that in addition to the kinetic fractionation of oxygen, significant oxygen exchange (O-exchange) occurs between H_2O and N_2O precursors. Incorporation of H_2O–O into N_2O was up to 94%. The magnitude of O-exchange was not influenced by temperature, soil moisture, or the rate of N_2O production. High levels of O-exchange acted to reduce δ^{18}O in the nitrate source, meaning that δ^{18}O-N_2O values were controlled largely by δ^{18}O-H_2O. Values of δ^{18}O in

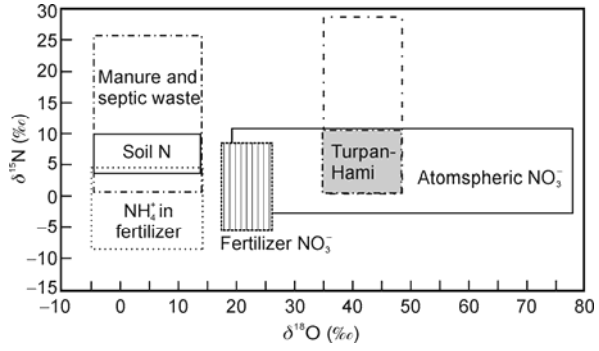

Figure 7 Range of δ^{18}O and δ^{15}N values for known nitrate sources [13].

atmospheric nitrate were abnormally high, whereas in water bodies $\delta^{18}O_{V\text{-}SMOW}$ values were low and the oxygen isotopes were in disequilibrium. Oxygen exchange between H_2O and N_2O reduces $\delta^{18}O$ values in the residual atmospheric nitrate, and even clears the anomaly of oxygen isotope. The high $\delta^{15}N$ and low $\delta^{18}O$ values in the Wuzongbulake niter deposits may have been caused by intense microbial denitrification and oxygen isotope exchange between H_2O–O and N_2O–O during the transport and evaporation of the nitrate.

The Dawadi niter deposit, where solid and liquid phases coexist, is a new salt lake and retains traces of the initial flooding. The source of the nitrate here may be older sodium deposits in the surrounding hills. The nitrate was transported only a short distance, and microbial denitrification was weak; consequently, $\delta^{15}N_{air}$ and $\delta^{18}O_{V\text{-}SMOW}$ are comparable to that of the source sodium nitrate deposits. This differs from the Wuzongbulake niter deposit. The $\delta^{18}O$ values of nitrate deposits in the Turpan-Hami Basin are generally lower than those from the Atacama Desert. Compared with values recorded in Death Valley, the $\delta^{18}O$ values of nitrate deposits in the Turpan-Hami Basin are much higher. The difference between them may be related to the proximity to the microbial denitrification.

2.3 Discussion for the mechanism

Due to the strong chemical bonds involved in NO_3^-, the transfer of oxygen isotopes between nitrate and water at normal temperatures is very difficult. Consequently, the original N and O isotope ratios of nitrates formed by photochemical reactions in the atmosphere are well preserved. The highly active gaseous NO_2 reacts readily with other materials to form nitrate aerosol particles that tends to be removed from the atmosphere by dry- or wet-deposition. Following its deposition, the former is transported by wind; the latter is transported with surface runoff and leaches into the subsurface.

In the middle Pleistocene, following local crustal uplift in this area, the previously cold, wet climate became drier, and by the late Pleistocene it was extremely dry [35–37]. Under these conditions of high evaporation, nitrate and other soluble salts that were deposited earlier and transported to surface in solution along capillary fissures in the gravel. Low-solubility salts (e.g., sulfate) saturate first, forming gypsum and other sulfates towards the base of the ore body; a small amount of darapskite may also have formed. High-solubility salts (e.g., chlorides and nitrates) continued to migrate upwards and became saturated in the upper ore body. A sodium nitrate belt was precipitated on the top of the ore body. Some of the nitrate minerals were transported long distances with the surface water to the basin center, where they evaporated to form a salt lake. After a long period of enrichment by evaporation and microbial action in the salt lake, the most highly soluble mineral, niter, was precipitated. Consequently, the niter deposits are younger than the sodium nitrate deposits. Optically stimulated luminescence (OSL) dating [38] and regional paleoclimatic records imply that the sodium nitrate ore deposits formed primarily during the late Pleistocene. Following this period, groundwater levels declined significantly, surface water was no longer available, and rates of mineralization subsequently decreased. However, capillary evaporation may have continued, allowing the formation of deposits in others areas.

3 Conclusions

In this paper, we have considered the distributions of oxygen and nitrogen isotopes, and their relationship with the ore-forming mechanism of the Turpan-Hami nitrate deposits in an attempt to improve the analytical methods used in nitrate purification. Levels of $\delta^{15}N$ were highly variable (0.7‰–27.6‰) but were mostly between 2‰ and 6‰, and this is similar to atmospheric NO_3^-. Levels of $\delta^{18}O$ were significantly elevated, with $\delta^{18}O_{V\text{-}SMOW}$ values ranging from 30.2‰ to 46.7‰ (mean value, 42.3‰). These values differ from other sources, but are similar to atmospheric NO_3^-. The nitrogen and oxygen isotope data indicate that the nitrate deposits in the Turpan-Hami Basin were created by the deposition of atmospheric nitrate particles. Different isotopic compositions of nitrogen and oxygen were found in the different types of deposit. The niter deposits showed elevated $\delta^{15}N_{Air}$ levels, but $\delta^{18}O_{V\text{-}SMOW}$ levels were significantly lower than in the sodium nitrate deposits. Both the sodium nitrate and the niter deposits have the same source. During the formation of the salt lake, and during nitrate transportation, the niter deposits experienced strong microbial denitrification. Using a combination of the geological context, paleoclimatic records, and analysis of the behavior of oxygen and nitrogen isotopes, we have identified the formation mechanisms of the different types of nitrate deposits in the Turpan-Hami region.

This study was supported by Basic Scientific Research Operation Cost of State-Leveled Public Welfare Scientific Research Courtyard (Grant No. K0926), National Natural Science Foundation of China (Grant Nos. 40543013, 40873003) and Key Laboratory of Isotope Geology, Ministry of Land and Resources.

1 Zhang Y M, Pan K Y, Zhao X S, et al. Nitrate deposits in the Xinjiang (in Chinese). Urumqi: Xinjiang University Press, 2000. 34–37, 73–81, 126–127
2 Ge W S, Qiu B, Sang S J, et al. Characters and genesis of Kumutage nitrate deposits in the Turpan-Hami, Xinjiang (in Chinese). Acta Mineral Sin, 2007, 27: 104–106
3 Gao Y Z. Composition and origin of soda nitre deposit in Shanshan Hongtai area, Xinjiang (in Chinese). Geol Chem Mine, 1993, 15: 17–24
4 Wang D S. Basis for the use of nitrogen isotopes to identify nitrogen contamination of groundwater (in Chinese). Acta Geosci Sin, 1997,

18: 221
5 Deng L, Cao Y Q, Wang W K. An overview of the study on nitrogen and oxygen isotopes of nitrate in groundwater (in Chinese). Adv Earth Sci, 2007, 22: 716–719
6 Sun J B, Deng Z F. Introduction of precipitation in the Xinjiang (in Chinese). Beijing: China Meteorological Press, 1987. 345–359
7 Li J F. Climate of the Xinjiang (in Chinese). Beijing: China Meteorological Press, 1991. 149–161
8 Ericksen G E. Geology and origin of the Chilean nitrate deposits-geological survey professional paper 1188. Washington DC: United States Government Printing Office, 1981. 1–37
9 Silva S R, Kendall C, Wilkison D H. A new method for collection of nitrate from freshwater and the analysis of nitrogen and oxygen isotope ratios. J Hydrol, 2000, 228: 22–36
10 Kendall C, Grim E. Combustion tube method for measurement of nitrogen isotope rations using calcium oxide for total removal of carbon dioxide and water. Anal Chem, 1990, 62: 526–529
11 Andersson K K, Hooper A B. O_2 and H_2O are each the source of one O in NO_2 produced from NH_3 by nitrosomonas: ^{15}N -NMR evidence. FEBS Lett, 1983, 164: 236–240
12 Hollocher T C. Source of the oxygen atoms of nitrate in the oxidation of nitrite by nitrobacter agilis and evidence against a P-O-N anhydride mechanism in oxidative phosphorylation. Archive Biochem Biophys, 1984, 233: 721–727
13 Michalski G, Böhlke J K, Thiemens M. Long term atmospheric deposition as the source of nitrate and other salts in the Atacama Desert, Chile: New evidence from mass-independent oxygen isotopic compositions. Geochim Cosmochim Acta, 2004, 68: 4023–4038
14 Kreitler C W. Nitrogen-isotope ratio studies of soils and groundwater nitrate from alluvial fan aquifers in Texas. J Hydrol, 1979, 42: 147–170
15 Mariotti A, Landeau A, Simon B. ^{15}N isotope biogeochemistry and natural denitrification process in groundwater: Application to the chalk aquifer of northern France. Geochim Cosmoch Acta, 1988, 52: 1869–1878
16 Mariotti A, Germon J C, Hubert P, et al. Experimental determination of nitrogen kinetic isotope fractionation: Some principes; illustration for the denitrification and nitrification processes. Plant Soil, 1981, 62: 413–430
17 Heaton T H E. Isotopic studies of nitrogen pollution in the hydrosphere and atmosphere: A review. Chem Geol Isot Geosci, 1986, 59: 87–102
18 Yoshinari T, Wahlen M. Oxygen isotope ratios in N_2O from nitrification at a waste water treatment facility. Nature, 1985, 317: 349–350
19 Wassenaar L I. Evaluation of the origin and fate of nitrate in the Abbotsford Aquifer using the isotopes of ^{15}N and ^{18}O in NO_3^-. Appl Geochem, 1995, 10: 391–405
20 Durka W, Schulze E D, Gebauer G. Effects of forest decline on uptake and leaching of deposited nitrate determined from ^{15}N and^{18}O measurements. Nature, 1994, 372: 765–767
21 Mayer B, Bollwerk S M, Mansfeldt T, et al. The oxygen isotope composition of nitrate generated by nitrification in acid forest floors. Geochim Cosmochim Acta, 2001, 65: 2743–2756
22 Liu C L, Wang M L, Jiao P C. Hydrogen, oxygen, strontium and sulfer isotopic geochemistry and potash-forming material sources of Lop salt lake, Xinjiang. Mine Deposits, 1999, (3): 268–275
23 Lehmann M F, Reichert P, Bernasconi S M, et al. Modelling nitrogen and oxygen isotope fractionation during denitrification in a lacustrine redox-transition zone. Geochim Cosmochim Acta, 2003, 67: 2529–2542
24 Böttcher J, Strebel O, Voerkelius S, et al. Using isotope fractionation of nitrate-nitrogen and nitrate-oxygen for evaluation of microbial denitrification in a sandy aquifer. J Hydrol, 1990, 114: 413–424
25 Aravena R, Robertson W D. Use of multiple isotope tracers to evaluate denitrification in ground water: Study of nitrate from a large-flux septic system plume. Ground Water, 1998, 36: 975–982
26 Mengis M, Schiff S L, Harris M, et al. Multiple geochemical and isotopic approaches for assessing ground water NO_3^- elimination in a riparian zone. Ground Water, 1999, 37: 448–457
27 Michalski G, Scott Z, Kailiing M, et al. First measurements and modeling of $\Delta^{17}O$ in atmospheric nitrate. Geophys Res Lett, 2003, 30: ASC14–1
28 Michalski G, Böhlke J K, Kendall C, et al. Isotopic compositions of Antarctic dry-valley nitrate: Implications for NO_x sources and cycling in Antarctica. Geophys Res Lett, 2005, 32: L13817
29 Savarino J, Kaiser S, Morin D, et al. Nitrogen and oxygen isotopic constraints on the origin of atmospheric nitrate in coastal Antarctica. Atomos Chem Phys, 2007, 7: 1925–1945
30 Campbell D H, Kendall C C, Chang C Y, et al. Pathways for nitrate release from an alpine watershed: Determination using $\delta^{15}N$ and $\delta^{18}O$. Water Resour Res 2002, 38: 10-1–10-8
31 Böhlke J K, Ericksen G E, Revesz K. Stable isotope evidence for an atmospheric origin of desert nitrate deposits in northern Chile and southern California, U.S.A. Chem Geol, 1997, 136: 135–152
32 Qin Y, Li Y H, Liu F, et al. Mass Independent Oxygen isotope fractionation in nitrate deposit of Xinjiang Turpan-Hami Area. Acta Geosci Sin, 2008, 6: 729–734
33 Li Y H, Qin Y, Liu F, et al. The discovery of mass independent oxygen isotopic compositions in super-scale nitrate mineral deposits from Turpan-Hami Basin, Xinjiang, China and its significance. Acta Geol Sin, 2010, 84: 1514–1519
34 Snider D M, Schiff S L, Spoelstra J. $^{15}N/^{14}N$ and $^{18}O/^{16}O$ stable isotope ratios of nitrous oxide produced during denitrification in temperate forest soils. Geochim Cosmochim Acta, 2009, 73: 877–888
35 Zheng X Y, Zhang M G, Li B X. Salt lakes in the Xinjiang (in Chinese). Beijing: Science Press, 1995. 141–142
36 Wen Q Z. The Quaternary Geology and Environment in the Xinjiang (in Chinese). Beijing: China Agriculture Press, 1994. 241–249
37 Pan A D. Preliminary study on vegetationial and climate evolution in Northern Xinjiang since the late Pleistocene (in Chinese). Arid Land Geogr, 1993, 6: 24–36
38 Qin Y. Nitrogen, oxygen isotopes characters and genesis of nitrate deposits of Turpan-Hami Area in the Xinjiang (in Chinese). Dissertation for the Doctoral Degree. Beijing: Chinese Academy of Geological Science, 2010. 70–73